Inorganic Chemistry

Communication

pubs.acs.org/IC

# Redox Modulation of Magnetic Slow Relaxation in a 4f-Based Single-Molecule Magnet with a 4d Carbon-Rich Ligand

Lucie Norel,*[,†] Min Feng,[†] Kevin Bernot,*[,‡] Thierry Roisnel,[†] Thierry Guizouarn,[†] Karine Costuas,[†] and Stéphane Rigaut*[,†]

[†]CNRS-Université de Rennes 1 and [‡]INSA Université Européenne de Bretagne, Institut des Sciences Chimiques de Rennes, UMR 6226, 263 Av. du Général Leclerc, F-35042 Rennes Cedex, France

Supporting Information

**ABSTRACT:** A ruthenium carbon-rich-based ligand that brings redox reversibility to a dysprosium-based single-molecule magnet is reported. Long-distance perturbation of the 4f ion is achieved upon oxidation, resulting in an overall enhancement of the magnetic slow relaxation.

Single-molecule magnets[1] (SMMs) are emerging as fascinating targets in the field of molecular spintronics[2] because they present a magnetic bistability at the scale of one molecule. The remote control of this property is currently a challenge with such molecular nanosystems.[2d] For example, the redox switching[3] of SMM would offer the attractive perspective of manipulating an individual magnetic molecule by means of an electrical potential.[4] For this purpose, only a few redox-active SMMs based on transition-metal complexes have recently been proposed.[5] In parallel, the use of highly anisotropic 4f ions has allowed the design of SMMs that display slow magnetic relaxation even at the scale of the single ion.[6] The redox control of such single-ion magnets (SIMs) necessarily involves the use of a redox-active ligand because most lanthanide ions possess only one available redox state (III). Scarce examples, from the family of phthalocyanine double-decker lanthanide complexes, show that electrochemical generation of an open-shell system on the phthalocyanine ligand is a promising way to modulate the hysteretic behavior of these 4f complexes.[7]

Another elegant way to explore the redox-switching ability of a 4f-based SIM would be to take advantage of its association with a carbon-rich ruthenium complex.[8] Indeed, these organometallic moieties are attractive redox-active building blocks that allowed commutation of different properties such as conductivity,[9] nonlinear optics[10] or luminescence.[11] This ability arises in such systems from the one-electron oxidation that creates a radical with a unique electronic structure because the spin density is delocalized on both the 4d ion(s) and the carbon-rich ligand(s).[12] In this work, we have taken advantage of this feature to achieve reversible redox modulation of the magnetic relaxation of a bimetallic ruthenium(II)−dysprosium(III) complex. We show that the redox event strongly impacts the magnetic behavior with evidence of the switching of a pure 4f SIM into a 4f−4d SMM with enhanced dynamical properties.

Recently, we reported a SIM decorated with a carbon-rich ligand that shows a $N_2O_6$ environment created by coordination of *trans*-[PhC≡C(dppe)$_2$RuC≡C-bipyridyl] [**1**; dppe = 1,2-bis(diphenylphosphino)ethane] to Dy(hfac)$_3$ (hfac$^-$ = hexafluoroacetylacetonate).[13] Unfortunately, dissociation of this complex (**2**) in electrolytic solutions precluded the study of its redox-switching abilities. We further anticipated that the replacement of hfac$^-$ groups by tta$^-$ (tta$^-$ = 2-thenoyltrifluoroacetonate), which presents a weaker electron-withdrawing effect, would increase the complex stability in polar media. We thus prepared the bimetallic complex **3** from [Dy(tta)$_3$·2H$_2$O] and **1** (see the Supporting Information, SI), as previously reported for the ytterbium analogue.[11]

The single-crystal X-ray diffraction (XRD) structure of **3** (Figure S2 and Tables S1−S3 in the SI) is very similar to that of **2** with a slightly distorted square-antiprism coordination polyhedron of the dysprosium (nearly $D_{4d}$ site symmetry), as confirmed by the continuous shape measures (CSM; Table S11 in the SI).[14] Therefore, the SIM behavior of **2** is likely to be maintained in **3**.[13] Whereas replacement of the hfac$^-$ ligands with tta$^-$ has very little influence on the structural features, it is crucial to achieving a stable redox switch. The cyclic voltammetry of **3** (Figure S3 in the SI) showed a reversible one-electron oxidation process with $E^\circ$ = 0.062 V ($\Delta E_p$ = 90 mV) versus $Cp_2Fe^{0/+}$ and an irreversible process at more positive potential ($E_{pa}$ = 1.0 V vs $Cp_2Fe^{0/+}$), which are assigned to the successive one-electron oxidations of the ruthenium acetylide moiety.[11] It is important to realize that even if 4f SIMs bearing redox-active ligands are known, very few convincing reports of their reversible oxidation exist.[7b,15] Indeed, stabilizing a cationic oxidized ligand in the environment of an electron-poor lanthanide $\beta$-diketonate moiety is challenging, and the ruthenium acetylide complexes are perfectly suitable for this purpose because the charge in the oxidized state is delocalized over the conjugated path.[12a]

The absorption properties of the **3**$^+$ state in the UV−vis−near-IR (NIR) and IR ranges were then investigated and showed the same features as the ytterbium analogue (Figure S4 and Table S4 in the SI).[11] In particular, a broad band in the NIR region ($\lambda$ = 1050 nm) characteristic of the oxidized ruthenium acetylide moiety was observed and reversibly switched ON and OFF when the applied potential was successively changed from 0 to 0.5 V. After the third cycle, the absorption was still over 90% of its initial value (Figure 1). In order to isolate **3**$^+$ for magnetic measurements, we performed chemical oxidation with an equimolar amount of acetylferrocenium tetrafluoroborate under inert conditions at −60 °C. After precipitation with pentane, the IR ($\nu_{C\equiv C}$ = 1906 cm$^{-1}$) and UV−vis (Figure S4 in

**Received:** December 16, 2013
**Published:** February 14, 2014

   dx.doi.org/10.1021/ic403081y | *Inorg. Chem.* 2014, 53, 2361−2363

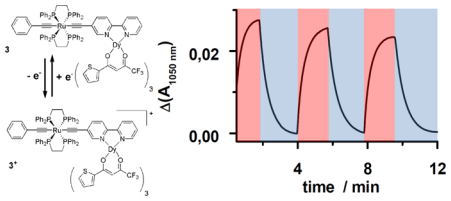


**Figure 1.** Evolution of absorbance at 1050 nm upon successive oxidations at 0.5 V (red) and reductions at 0 V (blue).

the SI) characteristics matched those obtained electrochemically and confirm full conversion to $[\mathbf{3}]\mathbf{BF_4}$. It remained stable at 77 K on the scale of hours, and the initial absorption spectrum could be obtained by further reduction with decamethylferrocene. All of this spectroscopic evidence shows reversible switching of the ruthenium acetylide fragment from a $S = 0$ state to a radical $S = {}^1/_2$ state, achieved both electrochemically and chemically.

The impact of oxidation on the magnetic properties could therefore be studied. First, the room temperature $\chi_M T$ value ($\chi_M T_{RT}$) for the neutral complex **3** is 14.27 emu·K·mol$^{-1}$, close to the expected value of 14.17 emu·K·mol$^{-1}$ for an isolated $Dy^{III}$ ion with $J = {}^{15}/_2$ and $g_j = {}^4/_3$ (Figure S6 in the SI). The $\chi_M T$ versus $T$ curves decrease as the temperature is lowered because of depopulation of the $J = {}^{15}/_2$ manifold that is split by the crystal field.[16] To characterize the ability of **3** to behave as a SIM, the dynamic magnetic properties, i.e., the in-phase ($\chi_M'$) and out-of phase ($\chi_M''$) components of the susceptibility, have been measured. In zero field, the $\chi_M''$ signal is observed at high frequencies only probably because of the occurrence of fast zero-field quantum-tunneling relaxation. This fast regime is suppressed as an external direct current field $H_{dc}$ is applied (Figure 2a), and a slow-relaxing regime is then promoted.[13] The most

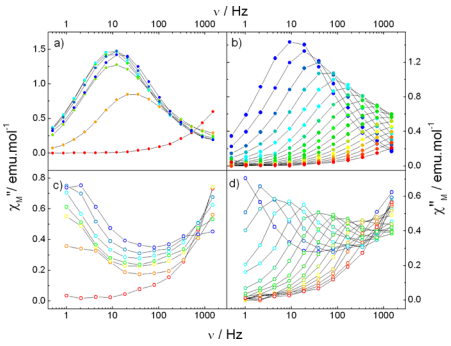


**Figure 2.** Frequency dependence of $\chi_M''$ for **3** (a) and $[\mathbf{3}]\mathbf{BF_4}$ (c) with $H_{dc}$ varying from 0 (red) to 1200 Oe (blue) and for **3** (b; dc field = 1000 Oe) and $[\mathbf{3}]\mathbf{BF_4}$ (d; $H_{dc}$ = 800 Oe) with the temperature varying from 2 (blue) to 6 K (red). Lines are guides to the eye.

efficient $H_{dc}$ field is evaluated to be 1200 Oe, and the relaxation frequency at 2 K ($\nu_{2\ K}$) is 12.4 Hz (Table 1). At this field, complex **3** shows temperature dependence of the magnetic relaxation in a wide range of temperature, which can be tentatively fitted considering an Arrhenius law for the relaxation time [$\tau = \tau_0 \exp(\Delta/k_B T)$] in the high-temperature range (Figure 3). The dynamic parameters are then estimated to be $\Delta = 32.8 \pm 1$ K and $\tau_0 = 1.15 \pm 0.2 \times 10^{-7}$ s (Tables 1 and S5 in the SI). Moreover, it can be noted that specific heat measurement does not show any evidence of phase ordering, thus confirming the single-molecule origin of slow relaxation (Figure S12 in the SI). Altogether, **3** shows in-field SIM behavior, which is very similar

**Table 1. Main Dynamic Parameters**

| | $\Delta^a$ (K) | $\tau_0$ (s) | relaxation frequency at 2 K (Hz) | $\alpha$ at 2.5 K |
|---|---|---|---|---|
| **3** | 32.8 | $1.15 \times 10^{-7}$ | 12.4 | 0.28 |
| $[\mathbf{3}]\mathbf{BF_4}$ | 43.5 | $0.46 \times 10^{-7}$ | 0.33 | 0.18 |

[a]Extracted from the high-temperature data. This value has to be considered with care because the Arrhenius plot is not in a strictly linear regime and because other relaxation processes can also be present (Raman and/or directprocess).

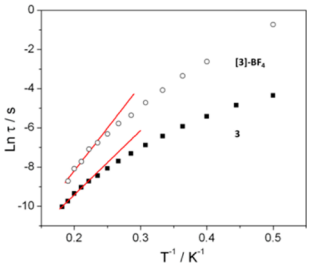


**Figure 3.** Arrhenius plots for **3** (squares) and $[\mathbf{3}]\mathbf{BF_4}$ (circles) with high-temperature best fits as lines.

to that of **2**, i.e., a double relaxation process with a slow regime enhanced by the application of a dc field.[13]

More challenging is characterization of the $\mathbf{3}^+$ state, given its limited stability at room temperature. Thus, $[\mathbf{3}]\mathbf{BF_4}$ was prepared (vide supra) in a sealed glass tube and immersed in a $N_2$ bath until its insertion into the magnetometer at low temperature (Figure S5 in the SI). The magnetic measurements (alternating-current and dc) were performed at low $T$ (<110 K), and fast switching of the temperature to 300 K was used to determine $\chi_M T_{RT}$ without decomposing the sample (Figure S6 in the SI). Again, in-field slow relaxation of magnetization is observed, with a lower optimum dc field of $H_{dc}$ = 800 Oe. Note that, for a given $H_{dc}$ field, the maximum in $\chi_M''$ is always observed at higher frequencies for **3** than for $[\mathbf{3}]\mathbf{BF_4}$ (Figure 2a,c). Therefore, at 2 K and with $H_{dc}$ = 800 Oe, complex $[\mathbf{3}]\mathbf{BF_4}$ relaxes significantly more slowly than **3** ($\nu_{2\ K}$ = 0.33 Hz; Table 1). In the entire investigated range of temperatures, $[\mathbf{3}]\mathbf{BF_4}$ shows also a slower relaxation than **3** (Figure 2b,d). To quantify this effect, a tentative extraction of $\Delta$ (Table 1) highlights that oxidation results in a 30% larger activation energy (43.5 K). Moreover, the Argand plots show that oxidation lowers the $\alpha$ value (from 0.28 to 0.18 at 2.5 K), thus reducing distribution of the relaxation times in the sample. Therefore, modification of the redox state of the organometallic moiety has an impact on the magnetic relaxation, which is significantly enhanced when the ruthenium acetylide fragment is in its radical-cation state.

To the best of our knowledge, this is the first time that such modulation of a heterobimetallic 4f–4d SMM is evidenced. We anticipated that either modification of the lanthanide crystal field or creation of an additional spin carrier upon oxidation could explain this modulation. An experimental structural determination of $\mathbf{3}^+$ is unfortunately not possible given the limited stability of cationic carbon-rich complexes in crystallization conditions, but some insight into the modulation process was obtained through a quantum-chemical study of the diamagnetic lutetium analogues **3-Lu** and $[\mathbf{3\text{-}Lu}]^+$ (see the SI).[17] First, the optimized geometry of **3-Lu** fits well with the square-antiprism symmetry of the lanthanide coordination sphere described earlier (Tables S9–S11 in the SI). In addition to the expected distance changes of the ruthenium acetylide part, oxidation also impacts


dx.doi.org/10.1021/ic403081y | Inorg. Chem. 2014, 53, 2361–2363

the lanthanide coordination sphere (Figure 4). Specifically, three Ln−O distances contract upon oxidation (−0.025 Å), while the

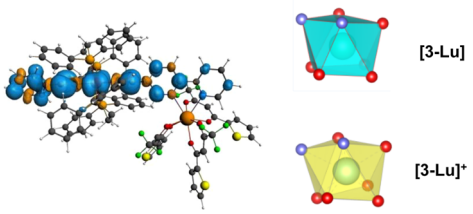


**Figure 4.** Isocontours of the spin density of [**3-Lu**]$^+$ (±0.0005 e·bohr$^{-3}$). Right: coordination spheres from optimized structures (density functional theory, DFT) of **3-Lu** and [**3-Lu**]$^+$ (nitrogen atoms in blue and oxygen atoms in red).

Ln−N bonds elongate (0.031 and 0.042 Å). This induces a small deformation in the lutetium coordination sphere, which is better described for [**3-Lu**]$^+$ as a triangular dodecahedron ($D_{2d}$) by CSM analysis (Table S11 in the SI). It has been demonstrated that repartition of the electrostatic charges around the lanthanide ions has a significant influence on their slow relaxation behavior.[18] A $Dy^{III}$ ion, in a free-ion approximation, is characterized by an oblate distribution of the f-orbital electronic density, and the lowest $M_J$ state is stabilized in the presence of an axial crystal field.[16] For **3**, electrostatic repulsion mainly originates from the six anionic oxygen atoms and is increased upon contraction of Ln−O distances. Thus, these modifications of the electrostatic environment of the $Dy^{III}$ ion may stabilize the lowest $M_J$ state and explain the observed increase of the activation barrier. It should also be considered that, for [**3-Lu**]$^+$, the calculated atomic spin density on the ruthenium center is only 0.48 e$^-$ so that there is an important polarized spin density on the conjugated chain with 10% of the atomic spin density on the bipyridyl group, including nitrogen-coordinating atoms (Figure 4). This fact suggests that, in the case of the paramagnetic lanthanide ions, a magnetic interaction of the 4f ion with the ligand could occur and influence the relaxation process.

In conclusion, this study shows for the first time reversible redox modulation of a SMM from a pure 4f to a 4d−4f state. The carbon-rich ruthenium unit, thanks to its unique electronic structure, brings redox reversibility to the system and produces an overall enhancement of the SMM properties upon oxidation. In addition, the chemical versatility of such carbon-rich complexes allows the design of an original extended structure and/or grafting on conducting surfaces. This opens up new horizons toward versatile molecular magnetic devices, the magnetic behavior of which could be tailored by external stimuli.

## ■ ASSOCIATED CONTENT

### Supporting Information

Experimental details for synthesis, a XRD study, SQUID measurements, DFT calculations, and a CIF file for **3**. This material is available free of charge via the Internet at http://pubs.acs.org.

## ■ AUTHOR INFORMATION

### Corresponding Authors

*E-mail: lucie.norel@univ-rennes1.fr.
*E-mail: kevin.bernot@insa-rennes.fr.
*E-mail: stephane.rigaut@univ-rennes1.fr.

### Notes

The authors declare no competing financial interest.

## ■ ACKNOWLEDGMENTS

We thank ANR (Grant ANR-09-JCJC-0025). This work was performed using HPC resources from GENCI-CINES and GENCI-IDRIS (Grant 2013-80649). We thank G. Poneti for his help with the magnetic measurements.

## ■ REFERENCES

(1) Gatteschi, D.; Sessoli, R.; Villain, J. *Molecular Nanomagnets*; Oxford University Press: Oxford, U.K., 2006.
(2) (a) Clemente-Juan, J. M.; Coronado, E.; Gaita-Arino, A. *Chem. Soc. Rev.* **2012**, *41*, 7464−7478. (b) Sanvito, S. *Chem. Soc. Rev.* **2011**, *40*, 3336−3355. (c) Bogani, L.; Wernsdorfer, W. *Nat. Mater.* **2008**, *7*, 179−186. (d) Timco, G. A.; Carretta, S.; Troiani, F.; Tuna, F.; Pritchard, R. J.; Muryn, C. A.; McInnes, E. J. L.; Ghirri, A.; Candini, A.; Santini, P.; Amoretti, G.; Affronte, M.; Winpenny, R. E. P. *Nat. Nano* **2009**, *4*, 173−178.
(3) Dul, M. C.; Pardo, E.; Lescouezec, R.; Chamoreau, L. M.; Villain, F.; Journaux, Y.; Ruiz-Garcia, R.; Cano, J.; Julve, M.; Lloret, F.; Pasan, J.; Ruiz-Perez, C. *J. Am. Chem. Soc.* **2009**, *131*, 14614−14615.
(4) (a) Komeda, T.; Isshiki, H.; Liu, J.; Zhang, Y.-F.; Lorente, N.; Katoh, K.; Breedlove, B. K.; Yamashita, M. *Nat. Commun.* **2011**, *2*, 217. (b) Lehmann, J.; Gaita-Arino, A.; Coronado, E.; Loss, D. *Nat. Nanotechnol.* **2007**, *2*, 312−317.
(5) (a) Newton, G. N.; Yamashita, S.; Hasumi, K.; Matsuno, J.; Yoshida, N.; Nihei, M.; Shiga, T.; Nakano, M.; Nojiri, H.; Wernsdorfer, W.; Oshio, H. *Angew. Chem., Int. Ed.* **2011**, *50*, 5716−5720. (b) Freedman, D. E.; Jenkins, D. M.; Iavarone, A. T.; Long, J. R. *J. Am. Chem. Soc.* **2008**, *130*, 2884−2885. (c) Soler, M.; Wernsdorfer, W.; Abboud, K. A.; Huffman, J. C.; Davidson, E. R.; Hendrickson, D. N.; Christou, G. *J. Am. Chem. Soc.* **2003**, *125*, 3576−3588. (d) Fortier, S.; Le Roy, J. J.; Chen, C.-H.; Vieru, V.; Murugesu, M.; Chibotaru, L. F.; Mindiola, D. J.; Caulton, K. G. *J. Am. Chem. Soc.* **2013**, *135*, 14670−14678.
(6) (a) Sessoli, R.; Powell, A. K. *Coord. Chem. Rev.* **2009**, *253*, 2328−2341. (b) Ishikawa, N.; Sugita, M.; Ishikawa, T.; Koshihara, S.; Kaizu, Y. *J. Am. Chem. Soc.* **2003**, *125*, 8694−8695. (c) Takamatsu, S.; Ishikawa, T.; Koshihara, S.-y.; Ishikawa, N. *Inorg. Chem.* **2007**, *46*, 7250−7252.
(7) (a) Ishikawa, N.; Sugita, M.; Tanaka, N.; Ishikawa, T.; Koshihara, S.-Y.; Kaizu, Y. *Inorg. Chem.* **2004**, *43*, 5498−5500. (b) Gonidec, M.; Davies, E. S.; McMaster, J.; Amabilino, D. B.; Veciana, J. *J. Am. Chem. Soc.* **2010**, *132*, 1756−1757.
(8) (a) Halet, J.-F.; Lapinte, C. *Coord. Chem. Rev.* **2013**, *257*, 1584−1613. (b) Low, P. J. *Coord. Chem. Rev.* **2013**, *257*, 1507−1532. (c) Ying, J.-W.; Liu, I. P.-C.; Xi, B.; Song, Y.; Campana, C.; Zuo, J.-L.; Ren, T. *Angew. Chem., Int. Ed.* **2010**, *49*, 954−957.
(9) Meng, F.; Hervault, Y.-M.; Shao, Q.; Hu, B.; Norel, L.; Rigaut, S.; Chen, X. *Nat. Commun.* **2014**, *5*, doi: 10.1038/ncomms4023.
(10) Green, K. A.; Cifuentes, M. P.; Samoc, M.; Humphrey, M. G. *Coord. Chem. Rev.* **2011**, *255*, 2530−2541.
(11) Di Piazza, E.; Norel, L.; Costuas, K.; Bourdolle, A.; Maury, O.; Rigaut, S. *J. Am. Chem. Soc.* **2011**, *133*, 6174−6176.
(12) (a) Costuas, K.; Rigaut, S. *Dalton Trans.* **2011**, *40*, 5643−5658. (b) Záliš, S.; Winter, R. F.; Kaim, W. *Coord. Chem. Rev.* **2010**, *254*, 1383−1396.
(13) Norel, L.; Bernot, K.; Feng, M.; Roisnel, T.; Caneschi, A.; Sessoli, R.; Rigaut, S. *Chem. Commun.* **2012**, *48*, 3948−3950.
(14) Casanova, D.; Llunell, M.; Alemany, P.; Alvarez, S. *Chem.—Eur. J.* **2005**, *11*, 1479−1494.
(15) Pointillart, F.; Guennic, B. L.; Golhen, S.; Cador, O.; Maury, O.; Ouahab, L. *Chem. Commun.* **2013**, *49*, 615−617.
(16) Rinehart, J. D.; Long, J. R. *Chem. Sci.* **2011**, *2*, 2078−2085.
(17) For the validity of the replacement of $Dy^{III}$ by a diamagnetic ion in DFT calculations, see, for example: Yi, X.; Bernot, K.; Le Corre, V.; Calvez, G.; Pointillart, F.; Cador, O.; Le Guennic, B.; Jung, J.; Maury, O.; Placide, V.; Guyot, Y.; Roisnel, T.; Daiguebonne, C.; Guillou, O. *Chem.—Eur. J.* **2014**, *20*, 1569−1576.
(18) Chilton, N. F.; Collison, D.; McInnes, E. J. L.; Winpenny, R. E. P.; Soncini, A. *Nat. Commun.* **2013**, *4*, doi: 10.1038/ncomms3551.